Characterization of New Cocrystals by Raman Spectroscopy, Powder X-ray Diffraction, Differential Scanning Calorimetry, and Transmission Raman Spectroscopy

ARTICLE *in* CRYSTAL GROWTH & DESIGN · MAY 2010

Impact Factor: 4.89 · DOI: 10.1021/cg100156a · Source: OAI

6 AUTHORS, INCLUDING:

Mohamed A Elbagerma
Misrata University
19 PUBLICATIONS **81** CITATIONS

SEE PROFILE

Michael D Hargreaves
Thermo Fisher Scientific
46 PUBLICATIONS **670** CITATIONS

SEE PROFILE

Pavel Matousek
Science and Technology Facilities Council
345 PUBLICATIONS **7,050** CITATIONS

SEE PROFILE

DOI: 10.1021/cg100156a

CRYSTAL GROWTH & DESIGN Article

XXXX, Vol. XXX 000–000

Characterization of New Cocrystals by Raman Spectroscopy, Powder X-ray Diffraction, Differential Scanning Calorimetry, and Transmission Raman Spectroscopy

M. A. Elbagerma,*,† H. G. M. Edwards,† T. Munshi,† M. D. Hargreaves,‡ Pavel Matousek,‡,# and I. J. Scowen†

†*Raman Spectroscopy Group, University Analytical Centre, Division of Chemical and Forensic Sciences, University of Bradford, West Yorkshire, BD7 1DP, U.K.,* ‡*Cobalt Light Systems Ltd, Start Electron, Fermi Avenue, Harwell Science & Innovation Campus, Didcot, Oxfordshire, OX11 0QR, UKU.K., and* #*Central Laser Facility, Science & Technology Facilities Council, Rutherford Appleton Laboratory, Oxfordshire, OX11 0QX, U.K.*

Received February 1, 2010; Revised Manuscript Received March 29, 2010

ABSTRACT: Cocrystals have been increasingly recognized as an attractive alternative delivery form for solids of drug products. In this work, salicylic acid was employed as a cocrystal former with the nicotinic acid, DL-phenylalanine, and 6-hydroxynicotinic acid (6HNA). Also, 3,4-dihydroxybenzoic acid with oxalic acid was studied. The cocrystals in all cases were prepared by slow evaporation from ethanol followed by characterization using Raman spectroscopy, powder X-ray diffraction, transmission Raman spectroscopy (TRS), and differential scanning calorimetry. Full understanding of the effects of formation on the vibrational modes of motion was obtained by the complete assignment of the spectra of the starting materials and of the cocrystal components. The results show that all the cocrystals, prepared in a 1:1 molar ratio, possess unique thermal, spectroscopic, and X-ray diffraction properties. Raman and TRS spectra showed that the vibrational modes of the cocrystal were different from those of the starting materials, suggesting that Raman spectroscopy and TRS are effective tools to evaluate cocrystal formation through interaction of their components. In addition, we have used a synthetic standard containing a 1:1:1 mixture of KNO_3 and raw material for which each sample was analyzed at seven random positions, with each point sampled twice. We have done the same with all cocrystals (1:1 KNO_3 and cocrystal), the ratios confirming that the cocrystal components (were in a 1:1 molar ratio).

1. Introduction

Cocrystallization is a crystallization method that allows the binding of two or more building blocks within one periodic crystal line lattice without making or breaking covalent bonds.[1] These building blocks are generally neutral molecular species linked via hydrogen bonds.[2] Cocrystals represent a class of unexplored compounds and offer huge opportunities for the pharmaceutical industry. Indeed, cocrystallization can be a new way to crystallize molecules that crystallize with difficulty in their pure forms or as salts. Pharmaceutical cocrystallization is a relatively recent technology which offers an alternative platform in improving the physicochemical properties of active pharmaceutical ingredients (APIs), such as the melting point, solubility, stability, and dissolution rate.[3]

APIs are complex chemical structures with functional groups that can take part in molecular recognition events. It is the presence of these functional groups, such as amides and carboxylic acids, that provides an ability to engage in supramolecular events with cocrystal formers having complementary hydrogen bond donor and acceptor sites, thereby forming pharmaceutical cocrystals.

The solid product of each reaction is commonly analyzed using X-ray powder diffractometry (PXRD) as the primary technique. PXRD detects changes in the crystal lattice and is therefore a powerful tool for studying polymorphism, pharmaceutical salts, and cocrystalline phases. PXRD can also be used as a component of automated robotic systems in high-throughput screening technologies.[4,5] However, drawbacks of this technique are the long measurement times, insensitivity toward isostructural crystals, and, for some materials, interference from preferred orientation effects; consequently, Raman spectroscopy is now being advocated as an analytical alternative to PXRD for cocrystal characterization.[6−8] Raman spectroscopy probes the effect of crystal structure on bond vibrational energies and is potentially able to selectively distinguish between the polymorphs of a given API. Furthermore, measurements are noninvasive, nondestructive, and rapid (data acquisition is achievable within seconds rather than minutes), which makes Raman spectroscopy ideal for automated high-throughput systems. Since Raman spectroscopy and PXRD are complementary techniques at the molecular level, in combination they can provide an increased understanding of solid-state phenomena. Also, the crystallization process and other physicochemical characteristics can be determined by differential scanning calorimetry (DSC) and infrared (IR).[9] On the other hand, Brittain has concluded that that the Raman spectroscopy is not useful in characterization of benzamide−benzoic acid cocrystal, though, Raman spectroscopy was found to be a useful vibrational spectroscopic technique for characterization of the benzylamine−benzoic acid system and benzenecarboxylic acids and their sodium salts systems.[10−12] Also, Elbagerma et al. have found that Raman spectroscopic is a very useful tool for characterization of benzamide−salicylic acid cocrystal.[13]

The principal benefit of transmission Raman spectroscopy (TRS) lies in its ability to provide rapid volumetric information

*To whom correspondence should be addressed.

on the content of pharmaceutical formulations including intact tablets and capsules eliminating the subsampling issues of conventional Raman spectroscopy and suppressing surface Raman and fluorescence components (e.g., from capsule shell or tablet coating). These features are important in quality control within a production environment.[14] From this point of view, the cocrystals were also analyzed with this method.

2. Experimental Section

2.1. Materials. Salicylic acid, nicotinic acid, DL-phenylalanine, oxalic acid, 6-hydroxynicotinic acid (6HNA), and 3,4-dihydroxybenzoic acid were purchased from Sigma-Aldrich at >98% purity. These materials were used as received. The solvent (ethanol) was HPLC grade and purchased from Reidel de Haën or Fisher Scientific.

Cocrystal formation was identified initially using Raman spectroscopy and the difference in melting points from the pure components and the structures were confirmed by X-ray diffraction.

2.2. Raman Spectroscopy. Raman spectra of the samples derived from the general preparative method described below as well as the

Scheme 1. The Starting Components of the Seven 1:1 Stoichiometry

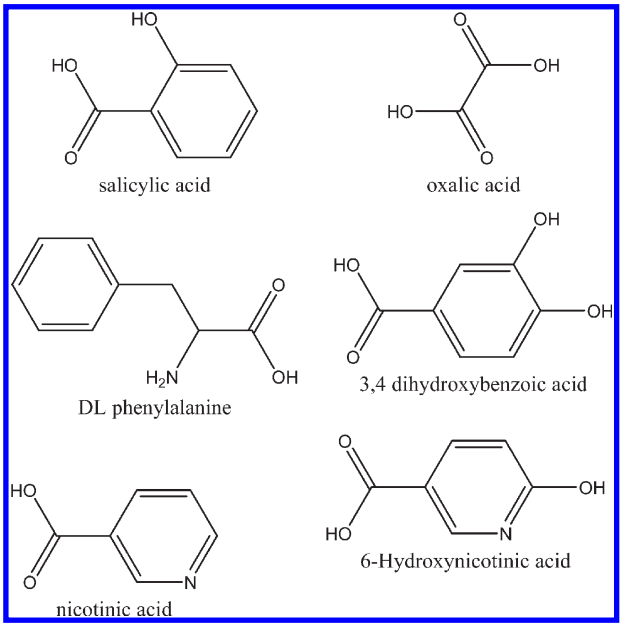

Table 1. Assignments of Major Bands of Raman Spectra of Salicylic Acid and Nicotinic Acid and Their 1:1 Cocrystal Products

salicylic acid	nicotinic acid	cocrystal	assignment[22−24]
3086		3070	7b (C−H) stretching
3075			2 (C−H) stretching
	3065		(C−H) stretching
	1694m	1675	*ν*(C═O)
		1672m	
1632s		1633m	C═O str
		1603m	
	1599s	1603	*ν4*(C═C)N
	1588m	1586m	*ν2*(C═C)N
1580m			8a
		1483w	
1471m		1471m	19a
1321s	1318m	1324 doublet broad	(C−O)c str
1306m	1306m	shoulder	*β*OH + *β*CH(9a) + vC-O)
1245s	1242w	1247m	(C−O)h str
1187m			
		1169m	
1163 m		1159s	3
1066w			13
	1113w		*β*CH(18b) + v(CC) + v(CN)
	1042s		*σ* ring (12) + *β*CH(18a)
		1036s	
	1031m		*σ* ring (12) + v ring (1)
1027s			18b
		850m	
		818m	
	810s		*σ* ring (6a) + v(C-X) + *σ* (COO)
805w			
		774s	
768s			
652w		652w	
	639w		*σ* ring (6b) + *σ* (COO)
564m		564m	
531m		531m	
449m		449w	
		439w	
385m			
	385 m		*ν*(C-X) + *σ* ring (6a) *σ* (COO)
		378w broad	
255m	255w	255s	
	204s	204w	
		182m	
177s			

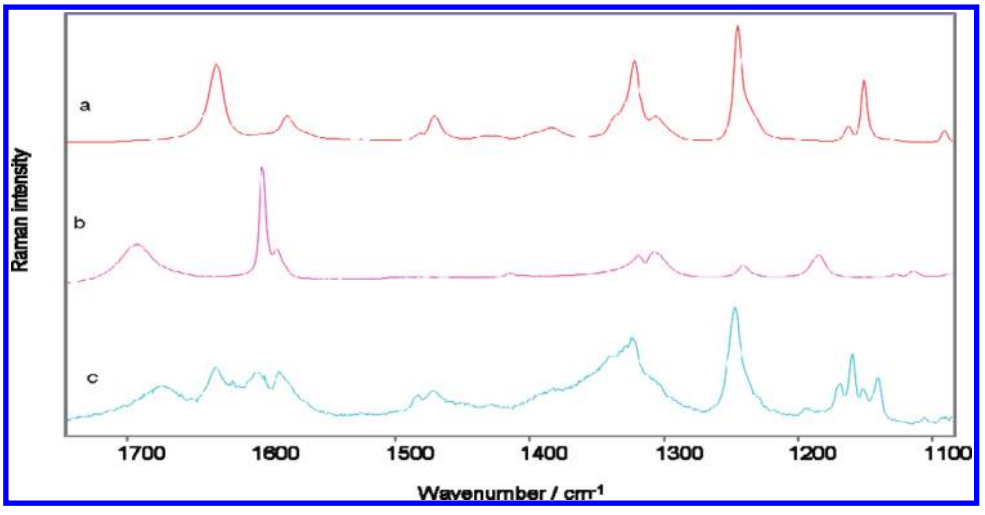

Figure 1. Raman spectra obtained for (a) salicylic acid, (b) nicotinic acid, and (c) the cocrystal.

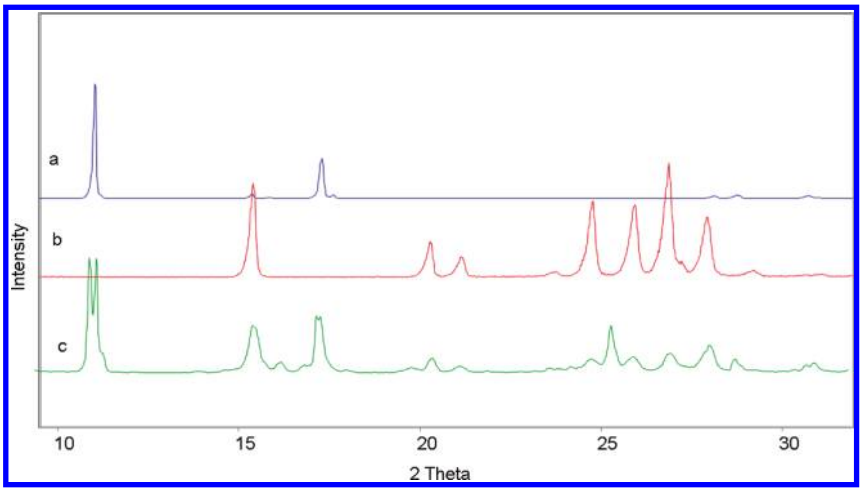

Figure 2. Powder X-ray diffraction patterns for (a) salicylic acid, (b) nicotinic acid, and (c) the cocrystal for full range.

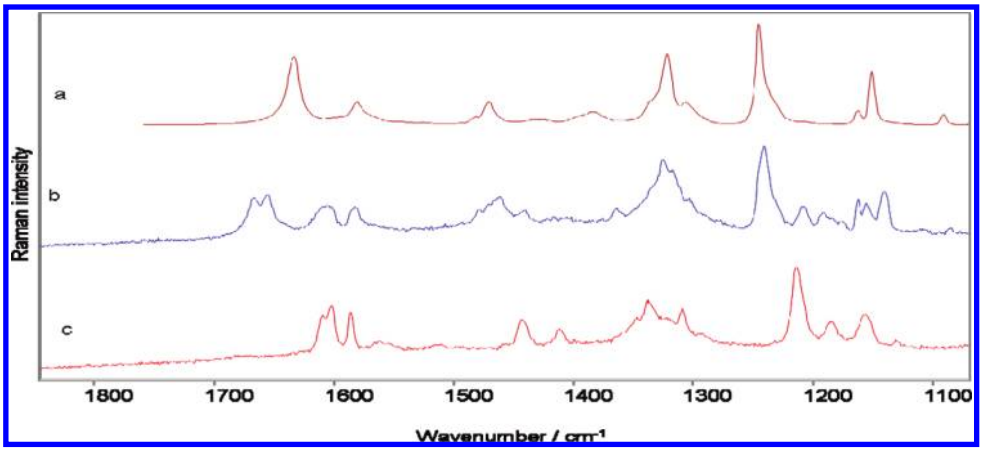

Figure 3. Raman spectra obtained for (a) salicylic acid, (b) the cocrystal, and (c) DL-phenylalanine.

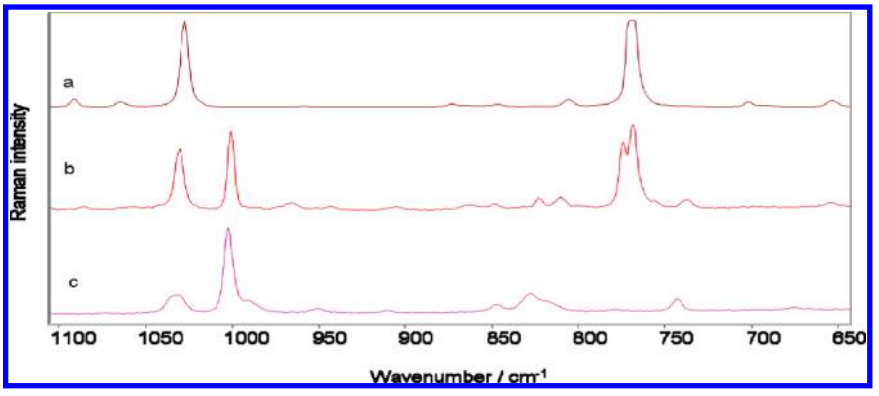

Figure 4. Raman spectra obtained for (a) salicylic acid, (b) the cocrystal, and (c) DL-phenylalanine.

single components were obtained using a Raman microscope (Renishaw plc.) with 785 nm stabilized diode excitation. The laser power at the sample was approximately 25 mW. A 50× objective lens was used, giving a laser spot diameter (footprint) of 2 μm at the sample. Spectra were obtained for a 10 s exposure of the CCD detector in the region 3600−50 cm^{-1} using the extended scanning mode of the instrument.

2.3. Transmission Raman Spectroscopy. Transmission Raman spectra were collected using a Cobalt Light Systems TRS100 dispersive Raman spectrometer. The vial was held in place (at an angle ~45°) and the excitation laser was directed onto the underside of the sample. Light was collected at ~180° from the direction of the excitation laser light, on the side of the vial. A NIR laser at 830 nm was used, with a power at the sample of approximately 1 W and a beam diameter of 3−4 mm. The imaging zone on the vial, determined by the collection optics, was 5 mm. All samples were measured for a 1 s exposure time, with 10 accumulations, giving a total scan time of 10 s. Transmission data were collected at a resolution of ~5−6 cm^{-1}, over the full dispersive range of the instrument ~45−2500 cm^{-1}.

2.4. Powder X-ray Diffraction. Data were collected on a Bruker D8 diffractometer in Bragg−Brentano $\theta-\theta$ geometry with Cu $K\alpha_{1,2}$ radiation (1.5418 Å) using a secondary curved graphite monochromator. The X-ray tube was operated at 40 kV, 30 mA. Samples were scanned in a vertical Bragg−Brentano ($\theta/2\theta$) geometry (reflection mode) from 5° to 40° (2θ) using a 0.005° step width

and a 1.5 s count time at each step. The receiving slit was 1° and the scatter slit 0.2°.

2.5. Differential Scanning Calorimetry. DSC profiles were generated in the range of 50 −160 °C using a TA Q2000 DSC instrument with an RGS90 cooling unit. Temperature calibration was performed using an indium metal standard supplied with the instrument at the appropriate heating rate of 10 °C min^{-1}. Accurately weighed samples (1−2 mg) were placed in Tzero aluminum pans using a similar empty pan as reference. The data were collected in triplicate for each sample and were analyzed using a TA Instruments Universal Analysis 2000 version 4.3A software.

2.6. Sample Preparation. Molecular structures of the cocrystal components used to prepare cocrystals 1−5 are illustrated in Scheme 1; experimental details of their preparation are presented below.

The standard method of preparation is exemplified as follows: salicylic acid (28.2 mg) and nicotinic acid (25.14 mg) were dissolved in 3 mL of ethanol. The mixture was warmed on a hot plate and the solution was allowed to cool to room temperature.

Slow evaporation of the solution resulted in the formation of a solid product which was isolated by filtration and air-dried. Similarly, for the other cocrystals: salicylic acid (28.2 mg) and DL-phenylalanine (33.73 mg) were dissolved in 3 mL of ethanol; salicylic acid (100 mg) and 6HNA (102.20 mg) were dissolved in 4 mL of ethanol; oxalic acid (100 mg) and 3,4 dihydroxybenzoic acid (171.19 mg) were dissolved in 5 mL of ethanol, and caffeine (100 mg) and 3,4 dihydroxybenzoic acid (79.36 mg) were dissolved in 5 mL of ethanol; they were also treated similarly to prepare their respective cocrystalline products.

3. Results and Discussion

The seven starting components have the following stoichiometry (Scheme 1).

3.1. Characterization of the Cocrystals. 3.1.1. Salicylic Acid and Nicotinic Acid (Vitamin B_3) Cocrystal. The Raman spectra of salicylic acid, nicotinic acid, and cocrystal are presented in Figure 1. The assignments for the most characteristic vibrational bands are listed in Table 1. Raman spectroscopic data were utilized first to evaluate whether the complex is a cocrystal or salicylic acid contains a carboxylic group and a hydroxyl group whereas nicotinic acid is a derivative of pyridine, with a carboxylic acid group (COOH) at the 3-position.

A comparison of the spectra reveals that there are several band shifts occurring between the individual components and the cocrystal; as shown in Figure 1, Table 1, the Raman spectra for pure nicotinic acid in the starting material have bands at 1694, 1599, and 1588 cm^{-1}, corresponding to ν(C═O), ν(C═C)N, and $\nu 2$(C═C)N, respectively. During the cocrystallization of nicotinic acid with salicylic acid, these bands in the cocrystal were shifted to 1675, 1603, and 1586 cm^{-1}, respectively. The decrease in the ν(C═O) frequency of nicotinic acid from 1694 to 1675 cm^{-1} and 1536 to 1533 cm^{-1} in the SA component indicates that the carbonyl group is participating in hydrogen bonding. The Raman spectra of pure salicylic acid and nicotinic acid have bands at 1321 cm^{-1} ((C−O) str) of the carboxylic group and 1318 cm^{-1}, respectively. During the cocrystallization, these bands appeared as a broad band at 1324 cm^{-1} as shown in Figure 1. Also, pure nicotinic acid spectrum has a band at 1306 cm^{-1}, corresponding to (βOH + βCH (9a) + νC−O)); through the cocrystal this band appears as a shoulder.

Upon cocrystallization, this band shifted to 1247 cm^{-1} with a decrease in the intensity; this observation indicates that the carboxylic group participates in hydrogen bonding. The peak at 1163 cm^{-1} in the spectrum of salicylic acid is shifted to 1159 cm^{-1} in the spectrum of the cocrystal and becomes stronger. Moreover, new bands at 1169 and 850 cm^{-1}, which do not occur in either salicylic acid or nicotinic acid, appear in the salicylic acid−nicotinic acid cocrystal.

Using a synthetic standard containing a 1:1:1 mixture of KNO_3, salicylic acid, and nicotinic acid for which each sample

Table 2. Assignments of Major Bands of Raman Spectra of Salicylic Acid, DL-Phenylalanine, and Their 1:1 Cocrystal Products

salicylic acid	DL-phenylalanine	cocrystal	assignment[20−28]
3086			7b (C−H) stretching
3075			2 (C−H) stretching
			(C−H) stretching
		1666m	
		1655m	
1632s			C═O str
	1609s	1607m broad	$[NH3]^+$ asym def; φ quad. ring str (ν_{8a})
	1602s		
	1585s	1582m	φ quad. ring str (ν_{8b}); $[NH3]^+$ sym def
1580m			8a
	1561w		COO^- asym. str.
	1510w		C−N asym str
1471m		1463m broad	19a
	1458w	disappear under 1463	φ s.c. ring str + CH def (ν_{19b})
	1442s	1441w	
	1411s	1410vw abroad	COO^- sym. str.
1383m		1363m	$(O-H)_h$ i.p. bend
	1346m	double broad	(O−H) i.p. def
	1337s	peaks 1325m,	
	1322m	1317m	φ sextant ring str. (ν_{14})
1321s			$(C-O)_c$ str
	1309s		CH_2 wagging
1306m		1301w	14
1245s		1240s	$(C-O)_h$ str
	1213vs	1207m	φ CH o.p. def (chain); CH_2 twist
	1185m	broad 1192, 1183,1175 vw	φ i.p. CH def (ν9a); C -O (H) str
1163 m		1162m	3
	1156s	1155m	φ i.p. CH def (ν_{15})
1151s		1139m	15
	1031s	1030s	C−C str
1027s			18b
	1002vs	1000vs	φ i.p. ring. def (ν_{12})
		965m	
	948m	941w	C−C str
	909w	903w broad	C−C str
	847m	847w	C−H out-of plane deformation
	827s	822w	C−C str
805w		811w	
	777vw	doublet 773,	C−C skeletal str
768s		768	
	742 m	737w	CH_2 rock
	726w		CH_2 rock
	618s	618w	φ i.p. ring. def (ν_{6b})
	602m	597vw	O C═O i.p. def
564m		560m	
531m		527w broad	
	518m		C C═O i.p. def; φ in. p. ring. def (ν_{6a})
		490w	
		478w	
	468m		COO^- rocking
449m		448w	
		438w	
385m			
	365m		σ(C−C), σ(C−C−C)
	313m	313w	C−C−C−C o. ph. def
255m		252w	
	208m	198w	lattice modes
177s		166,160m broad	

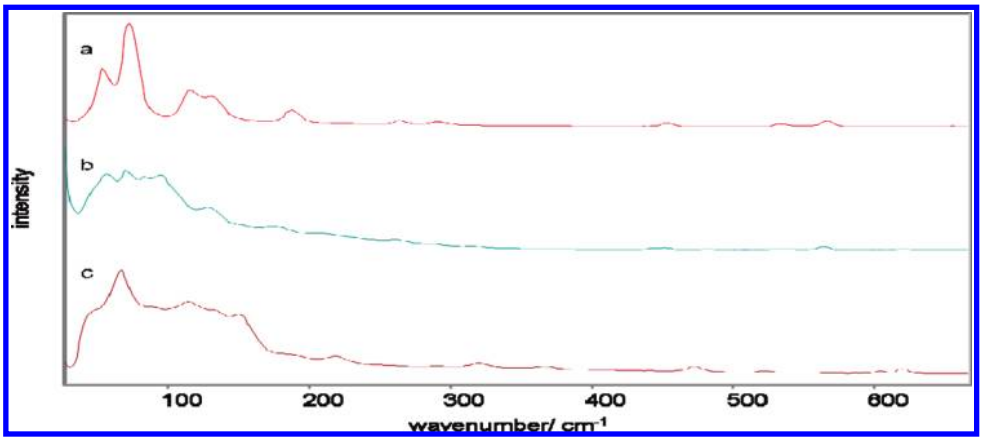

Figure 5. Transmission Raman spectra obtained for (a) salicylic acid, (b) the cocrystal, and (c) DL-phenylalanine.

Table 3. Major Bands of Transmission Raman Spectroscopy (TRS) of Salicylic Acid, DL-Phenylalanine, and their 1:1 Cocrystal Products

salicylic acid	DL-phenylalanine	cocrystal	assignment[24−28]
		1670m	
		1659m	
1632s			C═O str
	1611w	1606w broad	$[NH3]^+$ asym def; φ quad. ring str (ν_{8a})
	1604w		
	1580w	1582m	φ quad. ring str (ν_{8b}); $[NH3]^+$sym def
1583m			8a
	1561w		COO^- asym. str.
	1510w		C−N asym str
1473m		1465 m broad	19a
	1443w	1441w	
	1411w	1410 vw abroad	COO^- sym. str.
1385w		1365vw	$(O-H)_h$ i.p. bend
	1346m	double broad peaks	(O−H) i.p. def
	1337s	1325m, 1317m	
	1322m		φ sextant ring str. (ν_{14})
1321s			$(C-O)_c$ str
	1214m	1208w	φ CH o.p. def (chain); CH_2 twist
	1193w	1185w	φ i.p. CH def (ν9a); C−O (H) str
1163m		1162w	
	1158m	1156m	φ i.p. CH def (ν_{15})
1152s		1142m	15
1028vs		1031s	18b
	1028s		C−C str
	1003vs	1000s	φ i.p. ring. def (ν_{12})
	827w		C−C str
770w		770w	lattice modes
	217w		
188w		177w broad	
	149m		
132m		127m	
114w	114w		
		95m	
83m			
73s		71m	
	66s		
54m		57w	
	49w sh	48vwsh	

was analyzed at seven random positions, with each point sampled twice, the ratio of the 1599/768 cm^{-1} bands is 0.188; in the cocrystal the ratio of these bands is 0.195 confirming that it is a 1:1 cocrystal of salicylic acid and nicotinic acid.

The powder XRD diffractograms of the products of the specimen cocrystallized via slow evaporation from ethanol (Figure 2) show significant differences between the diffraction patterns of the raw material and the cocrystal product.

The DSC thermograms of nicotinic acid, salicylic acid, and their 1:1 cocrystal product are presented. The thermogram of salicylic acid shows a melting endotherm maximum at 159 °C and the thermogram of nicotinic acid shows a melting endotherm maximum at 236 °C. The DSC thermogram of the 1:1 stoichiometric product proved that the nicotinic acid−salicylic acid cocrystal had been formed; this substance exhibits a melting endotherm maximum at 128 °C.

3.1.2. Salicylic Acid and DL-Phenylalanine Cocrystal. The Raman spectra in the regions of 1800 to 1100, 1100 to 650, and 600 to 200 cm^{-1} for salicylic acid, DL-phenylalanine, and the salicylic acid−DL-phenylalanine crystal are presented in Figures 3 and 4. The assignments for the most characteristic vibrational bands are listed in Table 2. During the formation of the salicylic acid−DL-phenylalanine crystal, the OH and C═O bands of the salicylic acid are shifted to lower or higher wavenumber by 5−21 cm^{-1}, which suggests that the molecular complex of salicylic acid−DL-phenylalanine is a cocrystal.[15] The Raman spectrum for pure salicylic acid in the starting material has strong bands at 1632 cm^{-1}, 1245 cm^{-1} and a medium intensity peak at 1383 cm^{-1} corresponding to C═O stretching, ($(C-O)_h$ stretching (vibrational of hydroxylic group)) and ($(O-H)_h$ in-plane bending, respectively. During the cocrystallization, the band at 1632 cm^{-1} disappears and the bands at 1383 cm^{-1} and 1245 cm^{-1} shift to 1363 cm^{-1}, respectively. The disappearance of the C═O stretching mode and decrease in the ($(C-O)_h$ str, $(O-H)_h$) wavenumber of salicylic acid indicate that the carboxylic group is participating in strong hydrogen bonding. The peaks in the spectrum of DL-phenylalanine occurring at 1346 cm^{-1} ((O−H) in-plane deformation), 1337 cm^{-1}, 1322 cm^{-1}, and 1309 cm^{-1} (CH2 wagging) and the peak of salicylic acid at 1321 cm^{-1} ((C−O)c stretching (vibration of the carboxylic group)) appear as a bond doublet at 1325 and 1317 cm^{-1}.

The spectra of pure DL-phenylalanine have strong bands at 1609 corresponding to ($[NH3]^+$ asym deformation phenyl ring quadrant. ring str (ν8a)) and 1602 cm^{-1} appear as broad bands centered at 1582 cm^{-1} with decreased intensity. Also, the bands at 1411, 1213, and 1185 cm^{-1} correspond to (COO^- sym. str.), phenyl ring CH out of plane deformation (chain); CH_2 twist and phenyl ring in plane CH def (ν9a); C−O (H) str, respectively. During cocrystal formation, the strong band at 1411 cm^{-1} appears at 1410 cm^{-1} as a broad

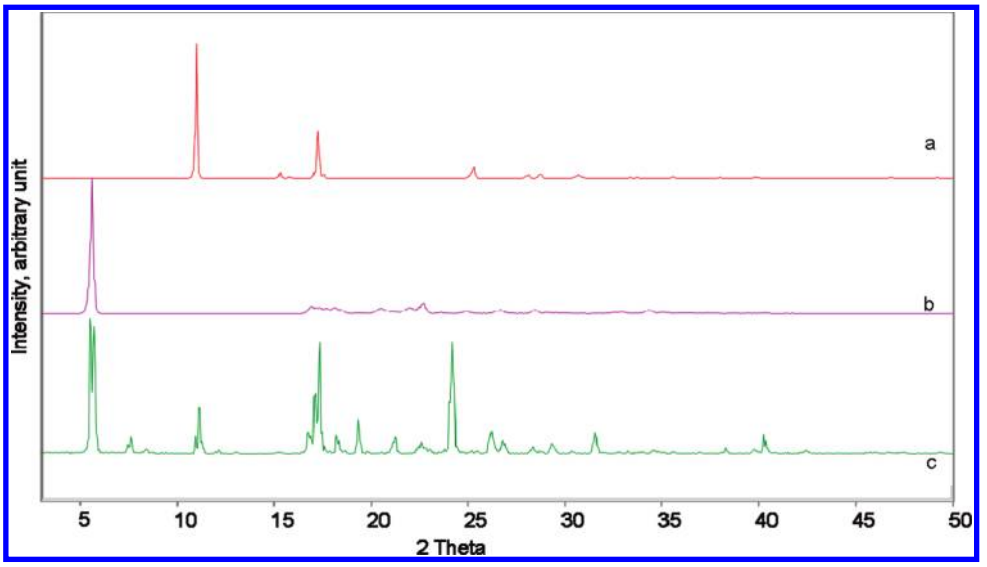

Figure 6. Powder X-ray diffraction patterns for (a) salicylic acid, (b) DL-phenylalanine, and (c) the cocrystal.

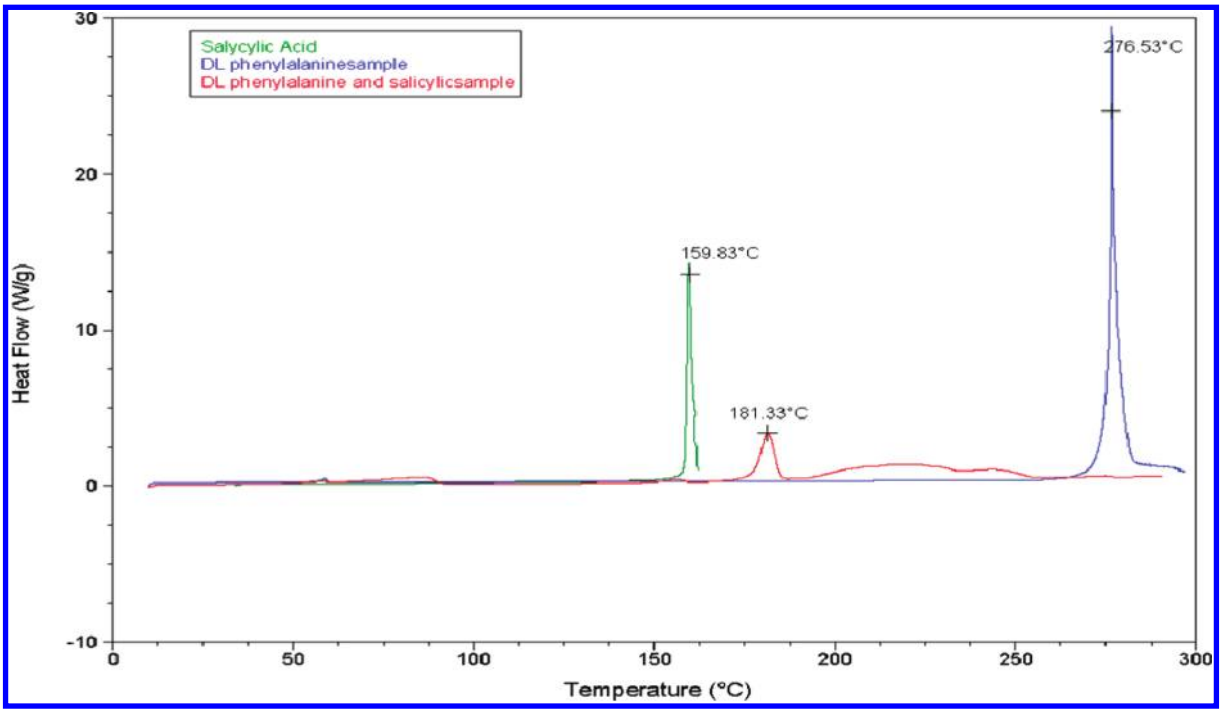

Figure 7. DSC melting curves of DL-phenylalanine (blue line), cocrystal (red line), and salicylic acid (green line).

very weak intensity band, the peak at 1213 cm^{-1} was shifted to 1207 cm^{-1} with decreased intensity, and the peak at 1185 cm^{-1} appeared as a weak broad peak at 1192, 1183, and 1175 cm^{-1}. These observations indicate that the amide and carboxylic groups are participating in strong hydrogen bonding.

On the other hand, new bands at 1666, 1655, 965, 940, and 478 cm^{-1} are not present in the pure reference spectra. Using a synthetic standard containing a 1:1:1 mixture of KNO_3, salicylic acid, and DL-phenylalanine for which each sample was analyzed at seven random positions, with each point sampled twice, the ratio of the 1213/1322 cm^{-1} bands is 0.381; in the cocrystal, the ratio of these bands is 0.375 confirming that it is a 1:1 cocrystal of salicylic acid and DL-phenylalanine.

Transmission Raman Spectroscopy (TRS). The transmission Raman spectroscopy (TRS) spectra of salicylic acid, the DL-phenylalanine, and the cocrystal are shown in Figure 5 and the vibrational wavenumbers and assignments are listed in Table 3.

The Raman spectrum of DL-phenylalanine in the starting material has bands at 1611, 1604, 1561, 1510, 1214, and 1193 cm^{-1}. In the cocrystal the bands at 1611 and 1604 cm^{-1} appear as a broad band at 1606 cm^{-1}; at the same time the other bands at 1561 and 1510 cm^{-1} have disappeared in the cocrystal and the bands at 1214 and 1193 cm^{-1} have shifted to lower wavenumbers at 1208 and 1185 cm^{-1}, respectively. The bands at 827, 217, and 149 cm^{-1} have disappeared in the cocrystal, while the peaks at 114 and 66 cm^{-1} have shifted to 127 and 71 cm^{-1}, respectively. On the other hand, the Raman

Table 4. Assignments of Major Bands of Raman Spectra of 3,4-Dihydroxybenzoic Acid, Oxalic Acid and Their 1:1 Cocrystal Products

oxalic acid	3,4-dihydroxybenzoic acid	cocrystal	assignment[29−33]
	3077w	3094vw broad	ν(CH)
	2584vw	2584vw 1792m	νOH
2584vw			νOH
1792m			
1778m			
1724s		1704 broad	νa (C═O)
	1604s	1616w	ν(CC)ar
	1599s	1604s	
	1514w		ν(CC)ar
1481m		1480w broad	δ(COH) + ν(C−O)
1454vw		1454vw	νs (C−O) + ν (C−C)
	1444w		CH3 bend C ring st
	1379w	1373m	CH3 bend C ring st.
	1364w		
	1338w		ν(OH) phenolic
	1291m	1313m	β(OH)carboxylic, (CC)ar
	1242m	1249m	CH bending
1173m			
	1097m		CO stretch (COOH)
	944m	944w	β(CH)
852w			νC−C)
837m		837s	νC−C)
824s		824m	
	794m	794w broad	
	771w		ring breathing
	754vs	761w	CH wagging
	636m		ring deformation
	593m		scissors (COOH)
541w		535w	
	531w		ring deformation
		478m	
463m			
455m			
449m			
	449m	429vw	ring wagging
	438m		
	382s	382vw	ring deformation
	343s	343w broad	OH wagging
	230m	225w broad	lattice mode
181s		174s	

spectrum for salicylic acid has bands at 1632, 1473, 1385, 1152, 1028, and 188 cm^{-1}. For the cocrystal, the peak at 1632 cm^{-1} has disappeared and the other peaks in the cocrystal were shifted to 1365, 1142, 1031, and 177 cm^{-1}, respectively. Moreover, new peaks at 1670, 1659, and 950 cm^{-1} are observed which do not occur in either salicylic acid or DL-phenylalanine.

PXRD patterns obtained for salicylic acid, DL-phenylalanine, and the stoichiometric 1:1 salicylic acid, DL-phenylalanine component are shown in Figure 6. The diffraction patterns of the three materials were found to be very different, with the product exhibiting characteristic peaks at 5.5, 15.7, 11.17, 19.34, and 24.23 deg 2θ, and salicylic acid exhibits characteristic peaks at 11.00 and 17.1 deg 2θ, whereas DL-phenylalanine exhibits characteristic peaks at 5.6 and 22 deg 2θ.

The DSC thermograms of benzamide, salicylic acid, and their 1:1 cocrystal product are presented in Figure 7 showing the thermogram of salicylic acid (melting endotherm maximum at 159 °C) and the thermogram of DL-phenylalanine (melting endotherm maximum at 276 °C). The DSC thermogram of the 1:1 stoichiometric product proved that the benzamide−salicylic acid cocrystal formed exhibits a melting endotherm maximum at 181 °C.

Table 5. Assignments of Major Bands of Raman Spectra of Salicylic Acid, and 6-Hydroxynicotinic Acid and Their 1:1 Cocrystal Products

salicylic acid	6-hydroxynicotinic acid	cocrystal	assignment[24,34−37]
	1717sh	1715w	
	1699s	1686w	C═O str
	1647m	1642s	ant(COOH)str
1632s			C═O str
	1622m	1622s	i.p. β(NH)
1583m		1583w	8a (C−C)str
	1554s	1555m	νas (CC/CN)
1473m		1468	19a (c-C)str
	1467s	1455sh	νas (CC/CN)
1383w			$(O-H)_h$ i.p. bend
		1355m	
		1343w	
	1335m	1337w	
1322s		1321vw broad	$(C-O)_c$ str
	1275vs	1265s	ν(C−O) str
	1254m	1257s	
	1237m	1231sh	
1245s		1243s	(C−O)h str
1163m			3
1152s		1156m	15(CC) i.p. bend
		1140m	
	1128w	1132w	
1026vs		1033s	18b(CC) i.p. bend
	859vs	doublet 859vs, 845s	
		846s	
806vw		795sh	12(CC) i.p. bend
772s		769s	
	768w		
	727w	722w	
	642w	doublet 638s, 635s	σ ring (6b) + σ (COO)
564s		559m	(O−H)c o.p. bend
	542m	541w broad	o.p. bend π (NH)
530m		527 broad	(C−O)h torsion
	512w	502w	
		477w	
	458w	450w	
448m		435m	9b
	402w	395m	
		332 broad	
255w		249 broad	10a
	256w		

3.1.3. 3,4-Dihydroxybenzoic Acid and Oxalic Acid Cocrystal. The molecular interaction between 3,4-dihydroxybenzoic acid and oxalic acid was examined by Raman spectroscopy, and the vibrational wavenumbers and assignments are listed in Table 4. The spectrum of oxalic acid showed a peak corresponding to the carbonyl νa(C═O) of carboxylic acid at 1724 cm^{-1}, The decrease in the C═O stretching wavenumber from 1724 cm^{-1} to 1704 cm^{-1} indicates that the carbonyl carboxylic group is participating in strong hydrogen bonding. This band was shifted in the Raman spectrum of the cocrystal to a lower wavenumber at 1704 cm^{-1} and appears as a broad peak as shown in Figure 8. The Raman spectra for pure oxalic acid in the starting material has bands at 1481 cm^{-1}, corresponding to the δ(COH) + ν(C−O), and 1173 cm^{-1}. During the cocrystallization of the oxalic acid with 3,4-dihydroxybenzoic acid, the band at 1481 cm^{-1} appears at 1480 cm^{-1} as a broad peak and the peak at 1173 cm^{-1} has disappeared in the cocrystal.

The Raman spectrum for pure 3,4-dihydroxybenzoic acid in the starting material has bands at 1604 cm^{-1} ν(CC)ar, 1599 and 1514 cm^{-1} ν(CC)ar. Upon cocrystallization, these bands in the cocrystal were shifted to 1616 cm^{-1}, 1604 cm^{-1} and disappear, respectively. Also, the bands at 1291 cm^{-1},

Table 6. Major Bands of Transmission Raman Spectroscopy (TRS) of Salicylic Acid, 6-Hydroxynicotinic Acid and Their 1:1 Cocrystal Products

salicylic acid	6-hydroxynicotinic acid	cocrystal	assignment[24,34−37]
	1702m	1686w	
	1651w		ant(COOH)str
1634s		1635 broad	C═O str
1583m		1583w	8a
	1557m	1557w	va,s (CC/CN)
	1510w		
1473m		1469m broad	19a
	1469m	1468m broad	va,s (CC/CN)
1386w		1386w broad	$(O-H)_h$ i.p.bend
	1337m	1342w broad	
1322m		1323w broad	$(C-O)_c$ str
1308m			14
	1277s	1268m	*v*(C−O) str
	1258w	1258m	
1246s		1246m	$(C-O)_h$ str
	1235m		
1152s		1152m broad	15 (C−C) i.p. bend
1028s		1028m	18b(C−C) i.p. bend
		938w broad	
	859s	doublet 859m, 848m	
769s		769s	
	643m	637m	σ ring (6b) + σ (COO)
		591w	lattice modes
188s		188w broad	
	155m		
132m		128m	
	120m		
115m			
	96s		
72s		72s broad	
53m		53w shoulder	
	46m		

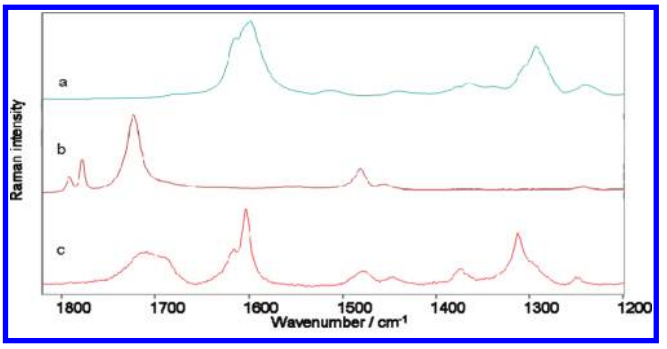

Figure 8. Raman spectra obtained for (a) 3,4-dihydroxybenzoic acid, (b) oxalic acid, and (c) the cocrystal.

1242 cm^{-1}, 1097 cm^{-1} and 754 cm^{-1}, corresponding to the β(OH)carboxylic, (CC)ar, CH bending, CO stretch (COOH), and CH wagging, respectively, and upon cocrystal formation, these bands were shift to higher wavenumbers with the exception of the band at 1097 cm^{-1}, which has disappeared.

Furthermore, the O−H stretching mode of the 3,4-dihydroxybenzoic acid shifted from 1291 to 1313 cm^{-1} in the cocrystal indicating that the intermolecular hydrogen bonds between 3,4-dihydroxybenzoic acid molecules were broken. Moreover, a new peak at 478 cm^{-1}, which does not occur in oxalic acid or 3,4-dihydroxybenzoic acid, is observed.

The Raman spectral data also confirmed that only oxalic acid is present in the complex, as no bands can be assigned to the oxalate[16] or hydrogen oxalate[17,18] ions. Furthermore, the v(C−C)stretching wavenumber, 837 cm^{-1}, is in agreement with that reported for $H_2C_2O_4$ molecule,[19] but this value is too low for $HC_2O_4^-$ or $C_2O_4^{-2}$ ions, where v(C−C) appears at about 880 cm^{-1}.[16−18]

Using a synthetic standard containing a 1:1:1 mixture of KNO_3, oxalic acid, and 3,4-dihydroxybenzoic acid for which each sample was analyzed at seven random positions, with each point sampled twice, and the ratio of the 834/754 cm^{-1} bands is 0.327; in the cocrystal the ratio of these bands is 0.329 confirming that it is a 1:1 cocrystal of oxalic acid and 3,4-dihydroxybenzoic acid.

The cocrystal formed between oxalic acid and 3,4-dihydroxybenzoic acid at a molar ratio of 1:1 was investigated by other solid-state analysis methods. The PXRD data for the oxalic acid−3,4-dihydroxybenzoic acid system are depicted in Figure 9. The PXRD pattern of the (oxalic acid−3,4-dihydroxybenzoic acid) differed from those of the constituents, confirming the formation of a new complex phase.

Furthermore, the DSC thermogram of the product exhibits a melting endotherm maximum at 96 and 159 °C providing further support for a new crystal phase. The thermal behavior of the new phase is significantly different from oxalic acid (melting endotherm maximum at 100.1 °C) 3,4-dihydroxybenzoic acid (melting endotherm maximum at 203 °C).

Transmission Raman Spectroscopy (TRS). The transmission Raman (TRS) spectra of oxalic acid, 3,4-dihydroxybenzoic acid, and the cocrystal are shown in Figure 10 and the vibrational wavenumbers are listed in Table 7.

The Raman spectrum for 3,4-dihydroxybenzoic acid in the starting material has bands at 1611 and 1299 cm^{-1}.

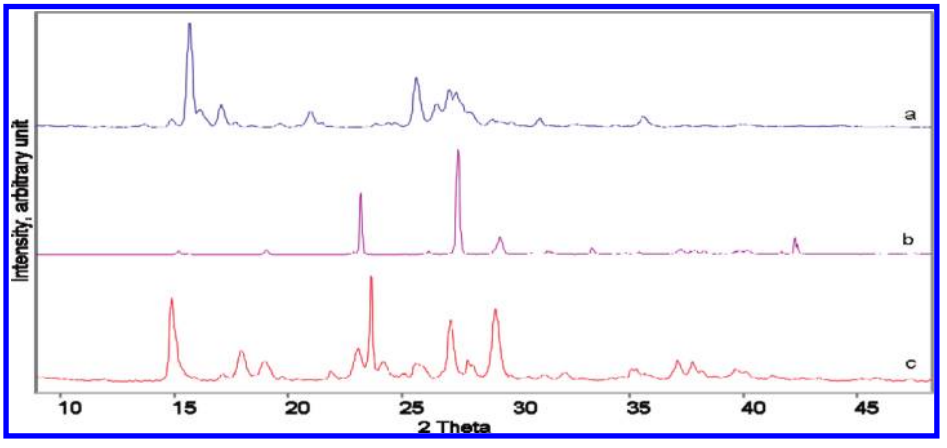

Figure 9. Powder X-ray diffraction patterns for (a) 3,4-dihydroxybenzoic acid, (b) oxalic acid, (c) and cocrystal.

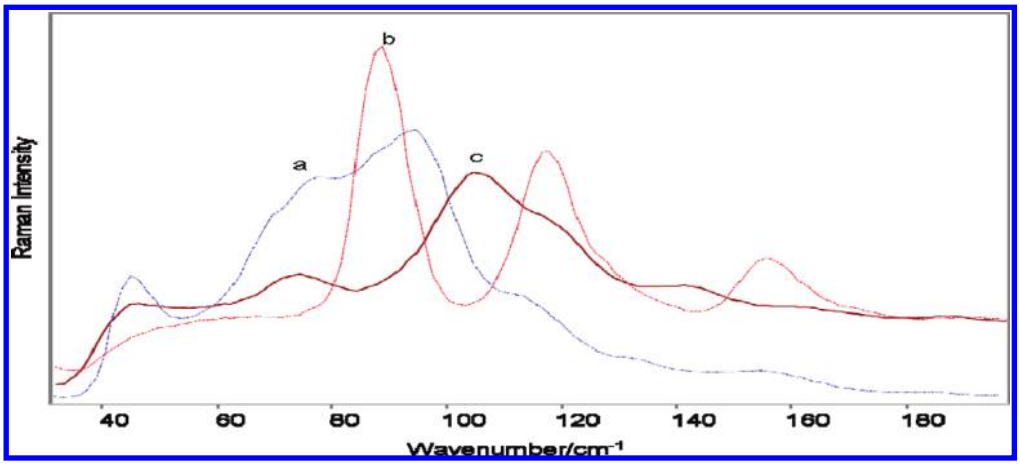

Figure 10. Transmission Raman spectra from 180 −40 cm^{-1} region obtained for (a) 3,4-dihydroxybenzoic acid, (b) oxalic acid, and (c) the cocrystal.

Table 7. Major Bands of Transmission Raman Spectroscopy (TRS) of Oxalic Acid, 3,4-Dihydroxybenzoic Acid and Their 1:1 Cocrystal Products[a]

oxalic acid	3,4-dihydroxybenzoic acid	cocrystal[29−33]
1796m		
1781m		
1725s		
1631w		
	1621sh	1620m
	1611s	1605s
	1299s	1315s
	1173m	
1156m		1155m
	1130w	
	1105s	
807m		791s
	797s	
543s		542 broad
448 broad		435m
	466s, 456s doublet	
362w		363w
	354s	348 broad
	243s	238s
456m		
156m		142m
117s		
	94s	
88vs		73m
	77s	

[a] vs, very strong; s, strong; m, medium; w, weak; vw, very weak; sh, shoulder; v, stretching; σ, scissoring; β in-plane deformation; a, antisymmetric; s, symmetric; as, asymmetric; i.p, in plane; o.p, out of plane; φ, phenyl ring; def, deformation; str, stretch.

These bands in the cocrystal were shifted to 1605 and 1315 cm^{-1}, respectively, while the peaks at 1173, 1130, and 1105 cm^{-1} disappear from the cocrystal spectrum. The Raman spectrum for pure oxalic acid has bands at 1796, 1725, 1156, and 543 cm^{-1}, whereas in the cocrystal the bands at 1796, 1725, and 1156 cm^{-1} have disappeared, and that band at 543 cm^{-1} is broadened but is still centered on 542 cm^{-1}. On the other hand, the peak at 156 cm^{-1} in the spectrum of pure salicylic acid has shifted to a lower wavenumber at 142 cm^{-1}.

3.1.4. Salicylic Acid and 6-Hydroxynicotinic Acid (6HNA) Cocrystal. The Raman spectra obtained in the fingerprint region for salicylic acid, 6HNA, and their cocrystal contained additional information regarding the intermolecular interactions associated with the cocrystal formation. Assignments for the observed Raman bands are collected in Table 6.

Raman spectra of the 6HNA, the in-plane β(C−OH) band is now missing at ca. 1280 cm^{-1}. Also, the strong band around 1023 cm^{-1}, attributed to the pyridine ring,[20] is not seen. These features suggest that the 6HNA could possibly have adopted the ketonic rather than the hydroxylated form. Furthermore, the presence of the v(C═O)stretching vibration at 1699 cm^{-1} and the in-plane β(NH) bend at 1622 cm^{-1} in the Raman spectra suggests that the ketonic form predominates in the solid state.[21]

The Raman spectrum for pure 6HNA in the starting material has bands at 1699 and 1467 cm^{-1} corresponding to C═O stretching and *va,s* (CC/CN), respectively; in the cocrystal formed between salicylic acid and 6HNA, these bands were shifted to 1686 and 1455 cm^{-1} and became shoulders. The decrease in the C═O stretching wavenumber of 6HNA from 1699 to 1686 cm^{-1} indicates that the carbonyl group is participating in hydrogen bonding. The Raman spectrum for pure salicylic acid in the starting material has strong bands at 1632, 1322 cm^{-1} and a medium intensity peak at 1383 cm^{-1} corresponding to C═O stretching, (C−O)c stretching and (O−H)h in plane bend, respectively. In the cocrystal, the band at 1632 cm^{-1} was shifted to 1642 cm^{-1}, the band at 1383 cm^{-1} disappears and the peak at 1322 cm^{-1} appears as a very weak broad band; these observations indicate that the carboxylic group is participating in hydrogen bonding as shown in Figure 11. The peaks in the spectrum of 6HNA occurring at 1275 cm^{-1} *v*(C−O) str, 1237 cm^{-1} and 642 cm^{-1} σ ring (6b) + σ (COO) in the cocrystal were shifted to 1265 cm^{-1}, 1231 cm^{-1} as a shoulder and a doublet at 638 and 635 cm^{-1}, respectively. Also, the peak at 859 cm^{-1} now appears as a doublet at 858 and 845 cm^{-1}. Furthermore, the Raman spectra for salicylic acid in the starting material has bands at 1163, 564, and 530 cm^{-1}, corresponding to (3)mode, (O−H)c o.p. bend and $(C-O)_h$ torsion, respectively. In forming the cocrystal, the band at 1163 cm^{-1} disappears and the other two bands were shifted to 559 cm^{-1} with (decreased intensity) and 527 cm^{-1} are broading, respectively.

Using a synthetic standard containing a 1:1:1 mixture of KNO_3, salicylic acid, and 6HNA for which each sample was analyzed at seven random positions, with each point sampled twice, the ratio of the 858:768 cm^{-1} bands is 0.479; in the cocrystal the ratio of these bands is 0.452 confirming that it is a 1:1 cocrystal of salicylic acid and 6HNA.

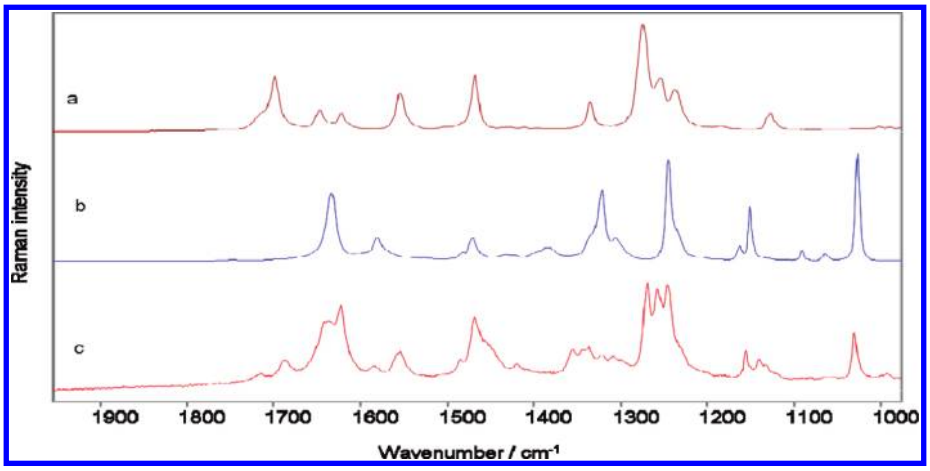

Figure 11. Raman spectra obtained for (a) 6-dihydroxynicotinic acid, (b) salicylic acid, and (c) the cocrystal.

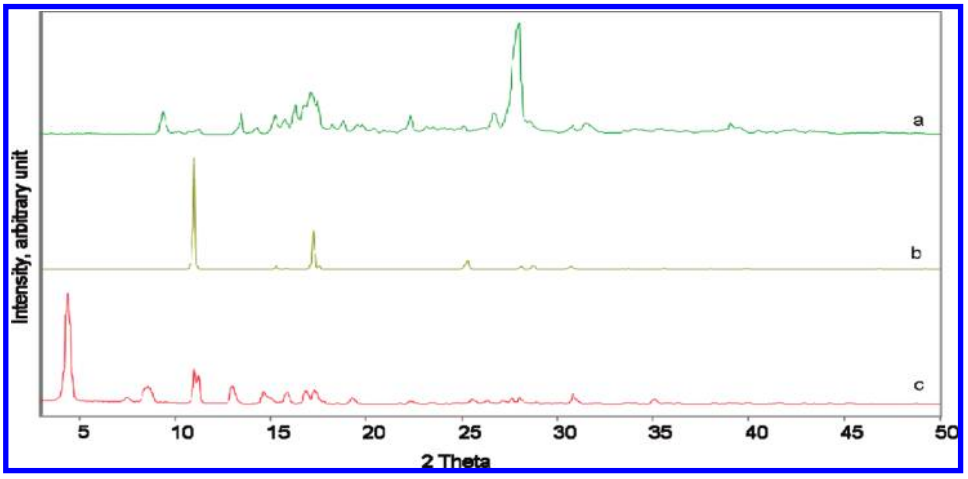

Figure 12. Powder X-ray diffraction patterns for (a) 6HNA, (b) salicylic acid, and (c) the cocrystal.

Scheme 2. Ketonic Form and Hydroxyl Tautomeric Form of 6HNA

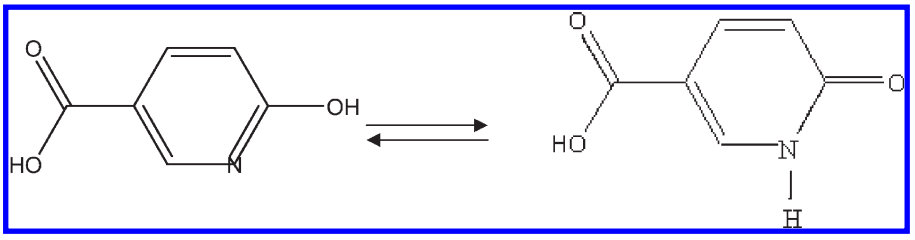

The powder XRD diffractograms of 6HNA, salicylic acid, and the product from their cocrystallization via slow evaporation from ethanol are compared in Figure 12. The intensity of the characteristic peaks at 27.9° and 11° of 6HNA and salicylic acid, respectively, were decreased during the cocrystal. Furthermore, the cocrystal has a strong peak at 4.42°, which indicated that a new phase was formed during the cocrystallization of 6HNA and salicylic acid.

Transmission Raman Spectroscopy (TRS). The TRS spectra of salicylic acid, 6HNA, and the cocrystal are shown in Figures 13 and 14 and the vibrational wavenumbers and assignments are listed in Table 6.

The Raman spectrum for 6HNA in the starting material has bands at 1702, 1651, and 1510 cm^{-1}. In the cocrystal the bands at 1651 and 1510 cm^{-1} have disappeared while that at 1702 cm^{-1} was shifted to lower wavenumber at 1686 cm^{-1}. The Raman spectrum for pure salicylic acid has bands at 1634, 1473, 1386, and 1322 cm^{-1}, corresponding to the C═O str, 19a, $(O-H)_h$ i.p. bend, and $(C-O)_c$ str, modes respectively. In the cocrystal formed between of salicylic acid with 6HNA, these bands appeared as broad bands at 1635, 1469, 1386, and 1323 cm^{-1}, respectively. On the other hand, the Raman spectrum for 6HNA has bands at 1235, 155, 120, 96, and 46 cm^{-1} which do not occur in the cocrystal. Also, the peak of medium intensity at 1308 cm^{-1} in pure salicylic acid has disappeared during the cocrystal formation. Moreover, new bands at 938 and 591 cm^{-1} which do not occur in either salicylic acid or 6HNA appear in the salicylic acid−6HNA cocrystal.

The DSC of 6HNA, salicylic acid, and cocrystallization product from slow evaporation are presented in Figure 15. The new molecular complex has melting points at 153 and 202 °C, while salicylic acid has a melting endotherm

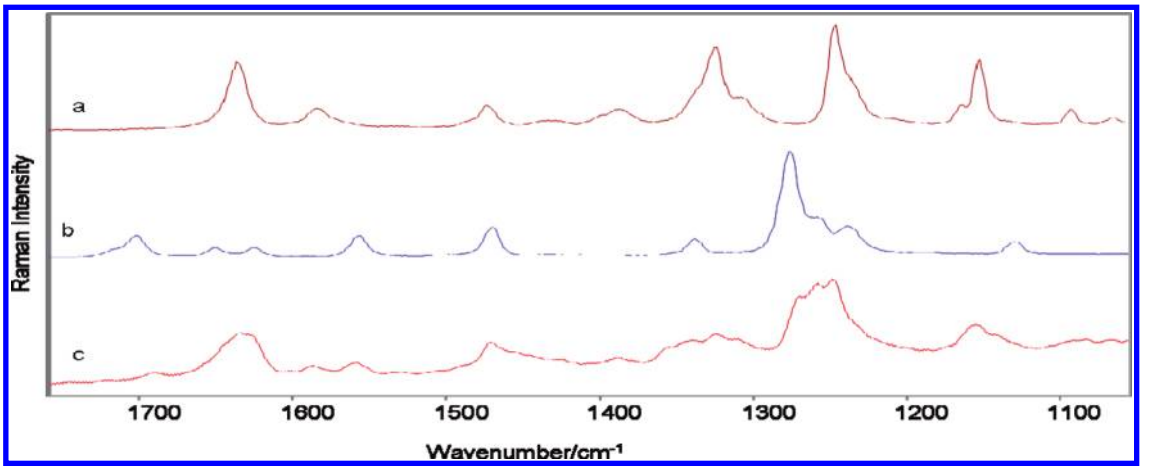

Figure 13. Transmission Raman spectra in the 1700−1100 cm^{-1} region obtained for (a) salicylic acid, (b) 6-hydroxynicotinic acid, and (c) the cocrystal.

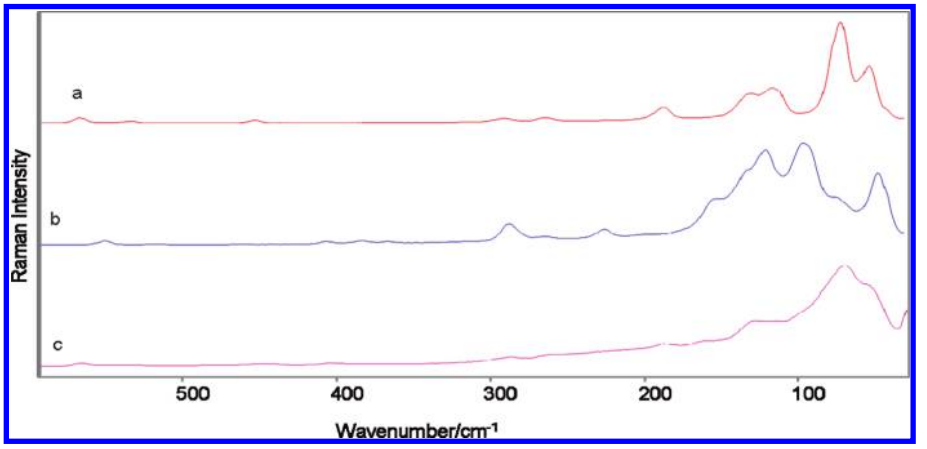

Figure 14. Transmission Raman spectra in the 500−100 cm^{-1} region obtained for (a) salicylic acid, (b) 6-hydroxynicotinic acid, and (c) the cocrystal.

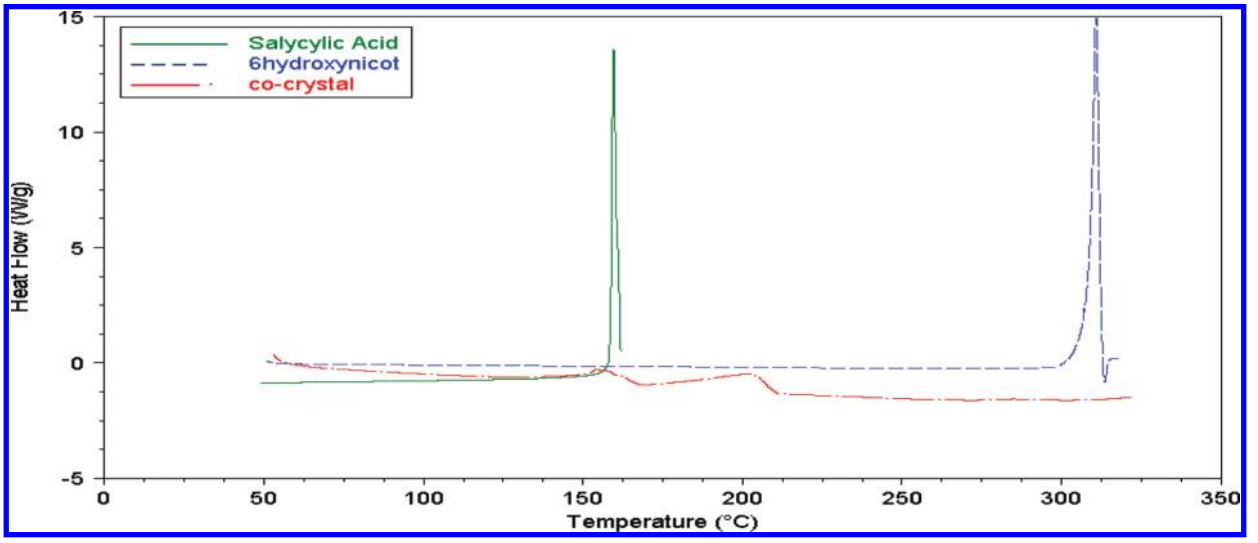

Figure 15. DSC melting curves of 6-hydroxynicotinic acid (blue line), cocrystal (red line), and salicylic acid (green line).

maximum at 160 °C and the 6HNA has a melting endotherm maximum at 300 °C.

4. Conclusions

The existence of salicylic acid−nicotinic acid, DL-phenylalanine, 6HNA, and 3,4-dihydroxybenzoic acid with oxalic acid cocrystals has been demonstrated in stoichiometric mixtures through the use of Raman spectroscopy (dispersive and transmission), X-ray powder diffraction and thermal analysis. Raman spectroscopy could be used to demonstrate a number of important aspects regarding the nature of the interactions in the cocrystal. Formation of the cocrystal causes broadening

in the carbonyl band region that is diagnostic for the existence of the cocrystals. Alterations in the energies of bands associated with the carbonyl vibrations of the carboxyl group were shown to be sensitive to fine details of the solids. The other main interaction point is the -OH group as it becomes deformed in the cocrystal. We have used a synthetic standard to confirm that the ratios of cocrystal components were in a 1:1 molar ratio.

TRS, which is well suited for rapid volumetric probing of intact samples, is applied to study cocrystals for the first time from which we can identify the presence of a different crystal structure in the cocrystal compared with the two precursor materials especially from low wavenumber Raman bands.

References

(1) Aakeroy, C. B.; Salmon, D. J. *CrystEngComm* **2005**, *7*, 439–448.
(2) Morissette, S. L.; Almarsson, O.; Peterson, M. L.; Remenar, J. F.; Read, M. J.; Lemmo, A. V.; Ellis, S.; Cima, M. J.; Gardner, C. R. *Adv. Drug. Delivery Rev*. **2004**, *56*, 275–300.
(3) Almarsson, O.; Zaworotko, M. J. *Chem. Commun*. **2004**, *17*, 1889–1896.
(4) Park, A.; Chyall, L. J.; Dunlap, J.; Schertz, C.; Jonaitis, D.; Stahly, B. C.; Bates, S.; Shipplett, R.; Childs, S. *Expert. Opin. Drug. Discovery* **2007**, *2*, 145–154.
(5) Storey, R.; Docherty, R.; Higginson, P.; Dallman, C.; Gilmore, C.; Barr, G.; Dong, W. *Crystallogr. Rev*. **2004**, *10*, 45–56.
(6) Morissette, S. L.; Soukasene, S.; Levinson, D.; Cima., M. J.; Almarsson, O. *Proc. Natl. Acad. Sci. U. S. A*. **2003**, *100*, 2180–84.
(7) Peterson, M. L.; Morissette, S. L.; McNulty, C.; Goldsweig, A.; Shaw, P.; LeQuesne, M.; Monagle, J.; Encina, N.; Marchionna, J. M.; Johnson, A.; Gonzalez-Zugasti, J.; Lemmo, A. V.; Ellis, S. J.; Cima, M. J.; Almarsson, O. *J. Am. Chem. Soc*. **2002**, *124*, 10958–10959.
(8) Hilfiker, R.; Berghausen, J.; Blatter, F.; Burkhard, A.; De Paul, S. M.; Freiermuth, B.; Geoffroy, A.; Hofmeier, U.; Marcolli, C.; Siebenhaar, B.; Szelagiewicz, M.; Vit, A.; Von Raumer, M. J. *Therm. Anal. Calorim*. **2003**, *73*, 429–40.
(9) Bolton, B. A.; Prasad, P. *Pharm. Sci*. **1984**, *73*, 1849–1851.
(10) Brittain, H. G. *Cryst. Growth Des*. **2009**, *9*, 2492–2499.
(11) Brittain, H. G. *Cryst. Growth Des*. **2009**, *9*, 3497–3503.
(12) Brittain, H. G. *Cryst. Growth Des*. **2010**, *10*, 1990−2003.
(13) Elbagerma, M. A.; Edwards, H. G. M.; Munshi, T.; Scowen, I. J. *Anal. Bioanal. Chem*. **2009**, DOI 10.1007/s00216-009-3375-7.
(14) Macleod, N. A.; Matousek, P. *Appl. Spectrosc*. **2008**, *62*, 276A–304A.
(15) Scott, M. G.; Henry, Y. I.; Loren, Z.; Mones, B. *J. Lipid Res*. **1981**, *l22*, 24–36.
(16) Socrates, G. *Infrared and Raman Characteristic Group Frequencies: Tables and Charts*, 3rd ed; John Wiley & Sons, Ltd: New York, 2001.
(17) Petrov, I.; Soptrajanov, B. *Spectrochim. Acta Part A* **1975**, *31*, 309–316.
(18) Villepin, J.; de Novak, A. *Spectrochim. Acta Part A* **1971**, *27*, 1259–1270.
(19) Villepin, J.; de Novak, A. *J. Mol. Struct*. **1976**, *30*, 255.
(20) Villepin, J.; de Novak, A. *Spectrochim. Acta Part A* **1971**, *34*, 1009–1017.
(21) Mukherjee, K. M.; Misra, T. N. *J. Raman Spectrosc*. **1996**, *27*, 595–600.
(22) Koczo, P.; Dobrowolski, J. C. Z.; Lewandowski, W.; Mazurek, A. P. *J. Mol. Struct*. **2003**, *655*, 89–95.
(23) Sala, O.; Gonçalves, N. S.; Noda, L. K. *J. Mol. Struct*. **2001**, *565−566*, 411–416.
(24) Volovsek, V.; Colombo, L.; Furic, K. *J, Raman Spectrosc*. **1983**, *14*, 347–352.
(25) Rajkumar, B.; Ramakrishnan, V. *Spectrochim. Acta Part A* **2002**, *58*, 1923–1934.
(26) Ramachandran, E.; Natarajan, S. *Cryst. Res. Technol*. **2007**, *42* (6), 617–620.
(27) Ravikumar, B.; Rajaram, R. K.; Ramakrishnan, V. *J. Raman Spectrosc*. **2006**, *37*, 597–605.
(28) Briget Mary, M.; Sasirekha, V.; Ramakrishnan, V. *Spectrochim. Acta Part A* **2005**, *62*, 446–452.
(29) Frost, R. L. *Anal. Chim. Acta* **2004**, *517*, 207–214.
(30) Godzisz, D.; Ilczyszyn, M.; Ilczyszyn, M. M. *Spectrochim Acta Part A* **2003**, *59*, 681–693.
(31) Mohacek-Grosev, V.; Grdadolnik, J.; Stare, J.; Hadzi, D. *J. Raman Spectrosc*. **2009**, *40* (11), 1605–1614.
(32) Kalinowska, M.; Swisłocka, R.; Borawskab, M.; Piekut, J.; Lewandowski, W. *Spectrochim. Acta Part A* **2008**, *70*, 126–135.
(33) Clavijo, E.; Menendez, J. R.; Aroca, R. *J. Raman Spectrosc*. **2008**, *39*, 1178–1182.
(34) Szorcsik, A.; Nagy, L.; Scopelliti, M.; Deak, A.; Pellerito, L.; Hegetschweiler, K. *J. Organomet. Chem*. **2005**, *690*, 2243–2253.
(35) Quintal, S. M.; Nogueira, H. I.; Felix, V.; Drew, M. G. *Polyhedron* **2002**, *21*, 2783–2791.
(36) Yin-Hua, H.; Zhi-Han, G.; Yun-Long, F. *Chin. J. Struct. Chem*. **2008**, *27* (9), 1073–1078.
(37) Xu, N.; Shi, W.; Liao, D.; Yan, S. *Inorg. Chem. Commun*. **2007**, *10*, 1218–1221.